

Corrosion Inhibition of Brass in Nitric Acid Using *Mimosa pudica* Seed Extract: Gravimetric, Electrochemical, Adsorption and Surface Characterization Studies

Tanvi Mahla*, M. B. Mahida**

*(Department of Chemistry, Atmanand Saraswati Science College, Varachha, Surat, Gujarat, India

Email: tanvimahla2410@gmail.com)

** (Department of Chemistry, Sir P. T. Sarvajani College of Science, Surat, Gujarat, India

Email: mbmahida@yahoo.com)

Abstract:

The corrosion behaviour of 62/38 brass in nitric acid and its inhibition by *Mimosa pudica* (Lajamani) seed extract were investigated using gravimetric, electrochemical, adsorption, and surface characterization techniques. Weight loss measurements showed that inhibition efficiency increased with inhibitor concentration (0.50–1.50 g L⁻¹) and decreased with increasing acid concentration (0.50–1.50 M) and temperature (303–323 K), indicating concentration-dependent and temperature-sensitive behaviour.

Adsorption of the inhibitor followed the Langmuir adsorption isotherm, suggesting monolayer formation on the metal surface. The calculated values of standard free energy of adsorption (ΔG°_{ads}) ranged from -18.95 to -24.32 kJ mol⁻¹, indicating spontaneous adsorption predominantly governed by physical interaction. The increase in activation energy in the presence of inhibitor further supported the formation of an energy barrier for the corrosion process.

Potentiodynamic polarization studies revealed a decrease in corrosion current density with a slight shift in corrosion potential, indicating that *Mimosa pudica* extract acts as a mixed-type inhibitor affecting both anodic and cathodic reactions. Surface characterization using SEM, EDX, AFM, and FTIR confirmed the formation of an adsorbed protective layer on the brass surface, although the film was not fully compact.

Overall, *Mimosa pudica* extract functions as a green corrosion inhibitor for brass in nitric acid through an adsorption-controlled mechanism, with moderate inhibition efficiency governed by predominantly physical adsorption.

Keywords — Brass, nitric acid corrosion, *Mimosa pudica* extract, green corrosion inhibitor, Langmuir adsorption isotherm, potentiodynamic polarization, surface characterization

I. INTRODUCTION

Brass, a copper–zinc alloy, is extensively used in industrial applications due to its favourable mechanical properties, thermal conductivity, and corrosion resistance in mild environments. However, its stability is significantly reduced in oxidising acidic media such as nitric acid, where rapid dissolution and dezincification occur due to enhanced anodic reactions and the absence of a stable passive film [1]. The presence of nitrate ions further accelerates corrosion by promoting

continuous metal dissolution and destabilising surface films [2].

Corrosion inhibition using organic compounds remains one of the most effective strategies for mitigating metal degradation in acidic environments. These inhibitors function primarily through adsorption at the metal–solution interface, forming a barrier that reduces charge transfer and limits the interaction between the metal surface and aggressive ions [3]. The efficiency of such inhibitors depends on molecular structure, presence of heteroatoms, electron density, and adsorption capability [4].

Conventional corrosion inhibitors, although effective, are often associated with environmental and health concerns due to their toxicity and low biodegradability [5]. Increasing regulatory pressure and environmental awareness have driven the development of green corrosion inhibitors derived from renewable and biodegradable sources [6]. Among these, plant extracts have gained considerable attention due to their availability, cost-effectiveness, and environmentally benign nature [7]. Plant-derived inhibitors contain a wide range of phytochemicals, including flavonoids, tannins, alkaloids, and phenolic compounds. These molecules possess functional groups such as hydroxyl, carbonyl, and aromatic rings, which facilitate adsorption onto metal surfaces through electrostatic interaction and donor-acceptor mechanisms [8]. The presence of π -electron systems enhances surface coverage, leading to suppression of both anodic metal dissolution and cathodic reactions [9]. Several studies have reported high inhibition efficiencies for plant extracts in acidic media, particularly for mild steel and copper-based alloys [10,11].

Despite extensive research on green inhibitors, studies involving nitric acid systems remain comparatively limited. Nitric acid presents a highly aggressive environment due to its strong oxidising nature, which promotes continuous corrosion and introduces competitive adsorption between inhibitor molecules and nitrate ions [12]. As a result, the adsorption behaviour becomes more complex, and many plant extracts exhibit reduced inhibition efficiency under such conditions [13]. Therefore, evaluation of inhibitors in nitric acid provides a more rigorous assessment of adsorption strength and film stability.

Recent studies have explored the use of agro-waste and plant-based materials as corrosion inhibitors, demonstrating their potential in reducing metal dissolution through adsorption-controlled mechanisms [14,15]. However, the performance of such inhibitors is strongly influenced by experimental parameters such as inhibitor concentration, acid strength, and temperature, which affect adsorption equilibrium and surface coverage [16].

Mimosa pudica (Lajamani) is a plant known for its rich phytochemical composition, including flavonoids, tannins, alkaloids, and phenolic compounds containing oxygen-rich functional groups [17]. These constituents provide multiple adsorption centres capable of interacting with metal surfaces. Although the plant has been widely studied for medicinal and biological properties, its application as a corrosion inhibitor, particularly for brass in nitric acid, has not been systematically investigated [18].

The present work aims to evaluate the corrosion inhibition behaviour of *Mimosa pudica* extract for 62/38 brass in nitric acid over a concentration range of 0.50–1.50 M. The study focuses on analysing the effect of inhibitor concentration and acid strength on corrosion rate, evaluating adsorption behaviour using isotherm models, and interpreting the inhibition mechanism based on thermodynamic and surface analysis. Unlike studies conducted in less aggressive media, this work emphasises inhibitor performance under oxidising conditions, providing a more critical understanding of adsorption stability and inhibition limitations [19,20].

II. MATERIALS AND METHODS

2.1 Materials

2.1.1 Brass Specimens

Commercial brass sheets with a nominal composition of 62 % Cu and 38 % Zn were used in the present study. Rectangular specimens of dimensions $4.5 \times 2.0 \times 0.2$ cm were prepared. A hole of approximately 5 mm diameter was drilled near the upper edge to facilitate suspension during immersion experiments. The effective exposed surface area of each specimen was 0.2097 dm^2 .

2.1.2 Surface Preparation

Prior to each experiment, the specimens were mechanically polished using successive grades of emery paper to obtain a smooth surface. The polished samples were rinsed thoroughly with double distilled water, degreased with acetone, and dried under ambient conditions. After immersion, corrosion products were removed using a standard cleaning procedure based on inhibited acid solution, followed by washing, drying, and reweighing. This

procedure ensures reproducibility and minimizes error in mass loss measurements [21].

2.1.3 Corrosive Medium

Analytical grade nitric acid (HNO_3 , 69%) was used to prepare solutions of 0.50, 0.75, 1.00, 1.25, and 1.50 M using double distilled water. All solutions were freshly prepared prior to use to avoid concentration variation. Nitric acid was selected due to its strong oxidising nature and its ability to induce rapid dissolution of brass, providing a stringent environment for evaluating inhibitor performance [22].

2.2 Preparation of Inhibitor

Seeds of *Mimosa pudica* (Lajamani) were used as the green corrosion inhibitor. The collected seed material was washed with distilled water to remove impurities, followed by shade drying and subsequent oven drying at 318–323 K to eliminate residual moisture. The dried material was ground into fine powder.

Extraction was carried out by refluxing 20 g of powdered seed material with 200 mL of 70% ethanol for 4 h. The extract was filtered, and the filtrate was concentrated using a water bath to obtain a semi-solid residue. The extract was further dried and stored in airtight conditions for subsequent use.

Test solutions were prepared by dissolving the required amount of extract in nitric acid solutions to obtain inhibitor concentrations in the range of 0.50–1.50 g L^{-1} . Ethanol-based extraction ensures efficient recovery of polyphenolic and oxygen-containing compounds responsible for adsorption on the metal surface [23].

2.3 Weight Loss Measurements

Gravimetric measurements were performed using 250 mL of test solution in glass beakers. Pre-weighed brass specimens were immersed in the solution for 24 h at 298 ± 1 K under static conditions. After immersion, the specimens were removed,

The experiments were conducted in 0.75 M HNO_3 at 298 ± 1 K. Prior to polarization measurements, the working electrode was allowed to stabilize at open circuit potential for 30 min.

Polarization measurements were performed over an appropriate potential range at a constant scan rate. The corrosion current density (I_{corr}), corrosion potential (E_{corr}), and Tafel slopes (β_a and β_c) were

cleaned to eliminate corrosion products, washed with distilled water, dried, and reweighed.

Corrosion rate (CR), inhibition efficiency (IE%), and surface coverage (θ) were calculated using standard gravimetric relations. Each experiment was conducted in triplicate, and the average values were reported to ensure reliability [24].

2.4 Effect of Temperature

Temperature dependent studies were carried out in 0.75 M HNO_3 over the temperature range 303–323 K with an immersion period of 3 h. A thermostatically controlled water bath was used to maintain constant temperature during experiments.

The corrosion rate values obtained at different temperatures were used to evaluate activation energy (E_a) using the Arrhenius equation and thermodynamic activation parameters based on transition state theory. Temperature variation provides insight into adsorption stability and the nature of interaction between inhibitor molecules and the metal surface [25].

2.5 Adsorption Studies

Surface coverage (θ) values were calculated from inhibition efficiency using the relation $\theta = \text{IE}/100$. The adsorption behaviour of *Mimosa pudica* extract on the brass surface was analysed using adsorption isotherm models.

The relationship between inhibitor concentration and surface coverage was examined to determine the nature of adsorption and interaction between inhibitor molecules and the metal surface. The applicability of the Langmuir adsorption isotherm was evaluated based on the linearity of the adsorption plots [26].

2.6 Potentiodynamic Polarization Measurements

Electrochemical studies were carried out using a conventional three-electrode system consisting of brass as the working electrode, Ag/AgCl as the reference electrode, and platinum as the counter electrode.

determined by extrapolation of anodic and cathodic branches.

The inhibition efficiency was calculated from the decrease in I_{corr} values. This method provides quantitative information on corrosion kinetics and inhibition mechanism [27].

2.7 Surface Characterization

2.7.1 SEM Analysis

Surface morphology was examined using scanning electron microscopy to evaluate corrosion damage and protective film formation [28].

2.7.2 EDX Analysis

Elemental composition was analysed to confirm adsorption of inhibitor species on the brass surface.

2.7.3 AFM Analysis

Surface topography and roughness parameters such as average roughness (Ra) and root mean square roughness (Rq) were evaluated.

2.7.4 FTIR Analysis

FTIR spectroscopy was used to identify functional groups responsible for adsorption of inhibitor molecules on the metal surface.

III. RESULTS AND DISCUSSION

3.1 Weight Loss Measurements

The corrosion behaviour of 62/38 brass in nitric acid in the absence and presence of *Mimosa pudica* (Lajamani) extract was evaluated using gravimetric measurements. The calculated corrosion rate (CR) and inhibition efficiency (IE%) values are presented in Table 1.

Table 1 Corrosion rate (CR, mg dm⁻² d⁻¹) and inhibition efficiency (IE, %) of *Mimosa pudica* extract for 62/38 brass in nitric acid solutions of different concentrations (0.50–1.50 M).

Green Inhibitor	Inhibitor Conc. (g L ⁻¹)	Acid Concentration									
		0.50 M		0.75 M		1.00 M		1.25 M		1.50 M	
		CR (mg dm ⁻² d ⁻¹)	I.E. (%)	CR (mg dm ⁻² d ⁻¹)	I.E. (%)	CR (mg dm ⁻² d ⁻¹)	I.E. (%)	CR (mg dm ⁻² d ⁻¹)	IE (%)	CR (mg dm ⁻² d ⁻¹)	IE (%)
Blank	–	1076	–	13066.	–	14809.	–	20556.	–	23639.	–
		7.07	–	83	–	76	–	10	–	02	–
<i>Mimosa pudica</i> (Lajamani)	0.50	4887	54.6	8383.7	35.8	10377.	29.9	15172.	26.1	18295.	22.6
		.60	2	6	3	65	2	46	8	62	0
	0.75	3992	62.9	7477.1	42.7	9485.0	36.0	13793.	32.9	16918.	28.4
		.33	1	3	8	9	0	92	0	44	6
	1.00	3307	69.2	6676.3	48.8	8597.6	41.9	12829.	37.6	15857.	32.9
		.61	9	5	9	7	5	32	1	32	1
	1.25	2780	74.1	6308.5	51.7	8154.8	44.9	12077.	41.2	15023.	36.4
		.47	7	7	0	3	4	62	3	63	4
	1.50	2402	77.6	6060.6	53.6	7913.1	46.5	11514.	43.9	14536.	38.5
		.98	9	0	4	2	8	83	8	79	0

In the absence of inhibitor, the corrosion rate increases markedly with increasing nitric acid concentration. The corrosion rate increases from 10767.07 mg dm⁻² d⁻¹ in 0.50 M HNO₃ to 23639.02 mg dm⁻² d⁻¹ in 1.50 M HNO₃, indicating the strong oxidising nature of nitric acid, where increased

nitrate ion concentration enhances anodic dissolution of both copper and zinc. The effect of nitric acid concentration on the corrosion rate is shown in Figure 1.

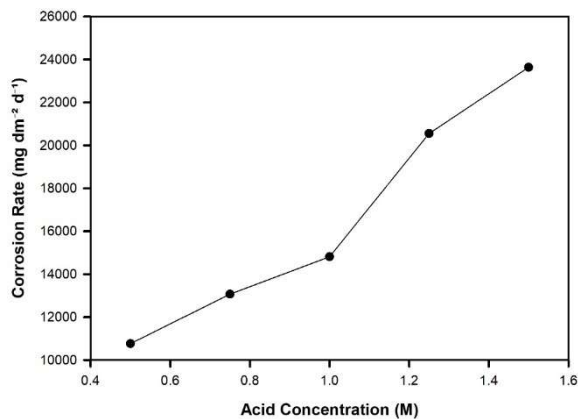


Figure 1 Effect of nitric acid concentration on the corrosion rate of 62/38 brass at 298 ± 1 K.

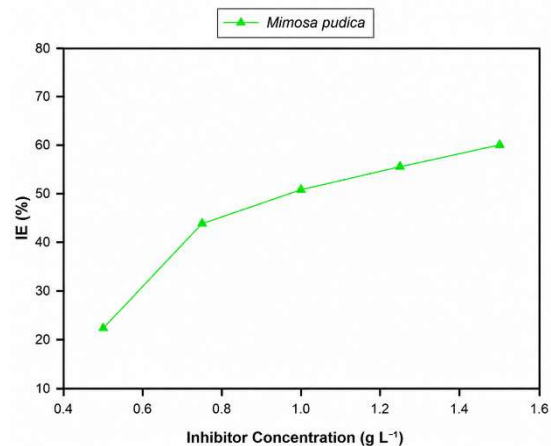


Figure 2 Effect of *Mimosa pudica* extract concentration (g L^{-1}) on inhibition efficiency (IE %) for 62/38 brass in 0.75 M HNO_3 at 298 ± 1 K.

In the presence of *Mimosa pudica* extract, the corrosion rate decreases at all acid concentrations, confirming its inhibitory action. However, the extent of reduction is moderate. At an inhibitor concentration of 1.50 g L^{-1} , the corrosion rate decreases to $2402.98 \text{ mg dm}^{-2} \text{ d}^{-1}$ in 0.50 M HNO_3 , corresponding to an inhibition efficiency of 77.69%. Under more aggressive conditions (1.50 M HNO_3), the corrosion rate remains relatively high ($14536.79 \text{ mg dm}^{-2} \text{ d}^{-1}$) with a lower inhibition efficiency of 38.50%.

A systematic decrease in inhibition efficiency with increasing acid concentration is observed across all inhibitor concentrations. For example, at 1.50 g L^{-1} , the inhibition efficiency decreases from 77.69% in 0.50 M to 38.50% in 1.50 M HNO_3 , indicating that adsorption becomes less effective in highly acidic media due to increased competition from nitrate ions. At constant acid concentration, the inhibition efficiency increases with increasing inhibitor. Overall, the results indicate that *Mimosa pudica* extract provides concentration-dependent corrosion inhibition for brass in nitric acid. The effectiveness is limited by acid strength, suggesting that adsorption is not sufficiently strong to maintain surface coverage under highly aggressive conditions.

concentration from 0.50 to 1.50 g L^{-1} . In 0.75 M HNO_3 , the inhibition efficiency increases from 35.83% to 53.64%, with a corresponding decrease in corrosion rate from 8383.76 to $6060.60 \text{ mg dm}^{-2} \text{ d}^{-1}$. The variation of inhibition efficiency with inhibitor concentration in 0.75 M HNO_3 is shown in Figure 2. The calculated surface coverage (θ) values increase with *Mimosa pudica* concentration, indicating progressive adsorption of inhibitor molecules on the metal surface. The variation of $\log(\theta / 1 - \theta)$ with concentration follows an ordered trend, supporting an adsorption-controlled inhibition mechanism.

Despite the increase in inhibition efficiency with concentration, the maximum efficiency does not exceed 77.69%, and decreases significantly at higher acid concentrations. This indicates comparatively weaker adsorption and less compact film formation by *Mimosa pudica* extract relative to more effective green inhibitors.

3.2 Effect of Temperature and Activation Parameters

The effect of temperature on the corrosion behaviour of 62/38 brass in 0.75 M HNO_3 in the absence and presence of *Mimosa pudica* (Lajamani) extract was investigated over the temperature range 303 – 323 K . The corrosion rate (CR), inhibition efficiency (IE%),

and activation energy (E_a) values are presented in Table 2.

Table 2 Effect of temperature (303–323 K) on corrosion rate (CR) and inhibition efficiency (IE, %) of *Mimosa pudica* extract for 62/38 brass in 0.75 M HNO_3 at different inhibitor concentrations.

Green Inhibitor	Inhibitor Conc. (g L^{-1})	Temperature (K)						Energy of activation (E_a) (kJ mol^{-1})			E_a from Arrhenius plot (kJ mol^{-1})
		303 K		313 K		323 K		303 K	313 K	323 K	
		CR ($\text{mg dm}^{-2} \text{d}^{-1}$)	I.E. (%)	CR ($\text{mg dm}^{-2} \text{d}^{-1}$)	I.E. (%)	CR ($\text{mg dm}^{-2} \text{d}^{-1}$)	I.E. (%)	Mean			
Blank	-	1061 8.00	-	15597 .00	-	21063. 00	-	30.2 8	25.2 1	27.7 5	27.88
<i>Mimosa pudica</i> (Lajamani)	0.50	8139 .94	23.3 5	11649 .88	25.2 8	15997. 59	24.0 5	27.0 0	28.0 0	27.5 0	27.30
	0.75	7009 .82	33.9 8	10559 .66	32.2 9	14654. 53	30.4 3	26.3 0	27.5 0	26.9 0	26.80
	1.00	5901 .67	44.4 1	9509. 61	39.0 1	13499. 72	35.9 0	25.6 0	26.7 0	26.1 5	26.00
	1.25	4919 .73	53.6 6	8439. 74	45.8 7	12359. 48	41.3 4	24.9 0	25.9 0	25.4 0	25.30
	1.50	4199 .85	60.4 5	7819. 63	49.8 6	11589. 74	44.9 6	24.2 0	25.2 0	24.7 0	24.60

In the absence of inhibitor, the corrosion rate increases significantly with temperature, indicating acceleration of electrochemical reactions due to increased thermal energy. The increase in corrosion rate reflects enhanced anodic dissolution of brass and increased kinetics of cathodic reactions in nitric acid medium.

In the presence of *Mimosa pudica* extract, a similar trend is observed; however, the corrosion rate values remain lower than those of the blank solution at all temperatures. This confirms that the inhibitor retains its protective effect over the studied temperature range, although the extent of inhibition decreases with increasing temperature.

At an inhibitor concentration of 1.50 g L^{-1} , the inhibition efficiency decreases with increasing temperature, indicating reduced adsorption stability at elevated temperatures. This behaviour suggests partial desorption of inhibitor molecules from the

metal surface, resulting in decreased surface coverage and increased exposure of active corrosion sites.

A consistent decrease in inhibition efficiency with increasing temperature is observed across all inhibitor concentrations, confirming that the protective film formed by the inhibitor is not stable at higher temperatures.

The temperature dependence of corrosion rate was analysed using the Arrhenius relationship. The corresponding plots of $\log \text{CR}$ versus $1/T$ are shown in Figure 3.

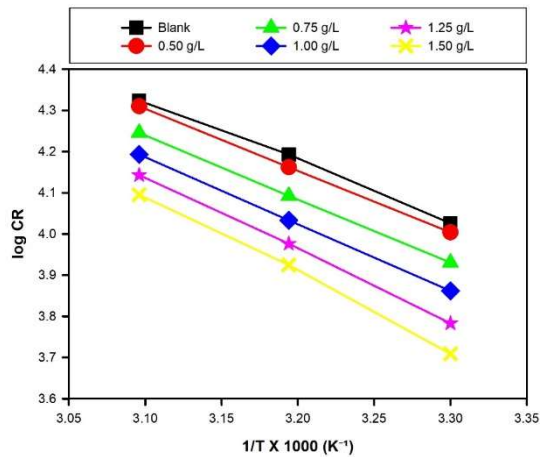


Figure 3 Arrhenius plots of log CR (mg dm⁻² d⁻¹) versus 1/T × 1000 (K⁻¹) for 62/38 brass in 0.75 M HNO₃ in the absence and presence of *Mimosa pudica* extract (0.50–1.50 g L⁻¹) over the temperature range 303–323 K after 3 h immersion.

The Arrhenius plots exhibit linear behaviour, confirming that the corrosion process follows Arrhenius kinetics. The activation energy (E_a) values increase in the presence of inhibitor compared to the blank solution.

The uninhibited system shows a lower activation energy, whereas in the presence of *Mimosa pudica*, the activation energy increases with increasing inhibitor concentration. This increase in activation energy indicates that the inhibitor introduces an energy barrier for the corrosion process, thereby reducing the rate of metal dissolution.

However, the magnitude of activation energy remains moderate, indicating relatively weak interaction between inhibitor molecules and the metal surface. The increase in activation energy, combined with the decrease in inhibition efficiency at higher temperatures, supports a mechanism involving predominantly physical adsorption.

In such systems, adsorption is relatively weak and sensitive to temperature, leading to partial desorption of inhibitor molecules at elevated temperatures. This behaviour is consistent with the moderate inhibition efficiency observed in weight loss measurements.

Overall, the temperature studies indicate that corrosion of brass in nitric acid is thermally activated and that the inhibition performance of *Mimosa pudica* extract decreases with increasing temperature. The results confirm that the protective film formed by the inhibitor is not highly stable at elevated temperatures, indicating limited adsorption strength.

3.3 Adsorption Isotherm

The inhibition of brass corrosion by *Mimosa pudica* (Lajamani) extract is attributed to adsorption of inhibitor molecules on the metal surface. To evaluate the adsorption behaviour, the experimental data obtained from weight loss measurements were analysed using the Langmuir adsorption isotherm. Surface coverage (θ) values were calculated from inhibition efficiency using the relation $\theta = IE/100$. The corresponding values of θ , $1-\theta$, and $\log(\theta / 1-\theta)$ at different inhibitor concentrations are presented in Table 3.

Table 3 Effect of inhibitor concentration (0.50–1.50 g L⁻¹) of *Mimosa pudica* extract on corrosion rate (CR), inhibition efficiency (IE, %), surface coverage (θ), and adsorption parameters for 62/38 brass in 0.75 M HNO₃.

Green Inhibitor	Inhibitor Concentration (g L ⁻¹)	CR (mg dm ⁻² d ⁻¹)	log CR	IE (%)	θ	1-θ	log(θ / 1-θ)
Blank	-	13066.83	4.1160	-	-	-	-
<i>Mimosa pudica</i> (Lajamani)	0.50	8383.76	3.9238	35.83	0.3583	0.6417	-0.2534
	0.75	7477.13	3.8737	42.78	0.4278	0.5722	-0.1263
	1.00	6676.35	3.8241	48.89	0.4889	0.5111	-0.0193
	1.25	6308.57	3.8002	51.70	0.5170	0.4830	0.0297
	1.50	6060.60	3.7824	53.64	0.5364	0.4636	0.0635

The adsorption behaviour of the inhibitor can be described using the Langmuir adsorption isotherm:

$$C/\theta = 1/K_{ads} + C$$

where C is the inhibitor concentration and K_{ads} is the adsorption equilibrium constant.

The plots of C/θ versus C are shown in Figure 4.

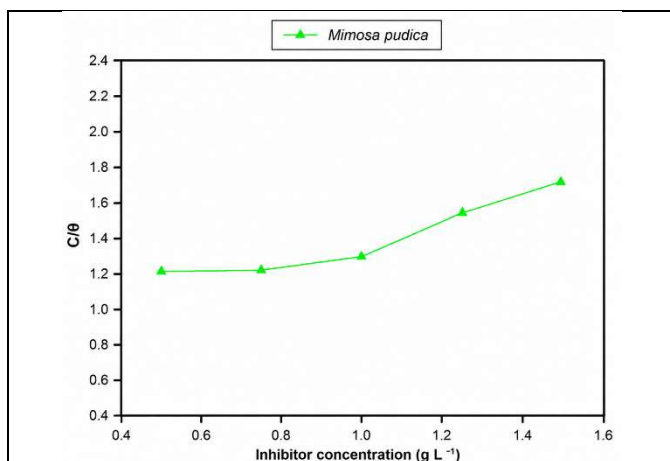


Figure 4 Langmuir adsorption isotherms (C/θ versus C) for *Mimosa pudica* extract on 62/38 brass in 0.75 M HNO₃ at 298 ± 1 K.

The linear relationship obtained from the plots, with slopes close to unity, indicates that the adsorption of *Mimosa pudica* extract on the brass surface follows the Langmuir adsorption isotherm. This suggests monolayer adsorption of inhibitor molecules on a relatively homogeneous metal surface with negligible interaction between adsorbed species.

However, slight deviations from ideal linearity are observed, which may be attributed to surface heterogeneity and competitive adsorption between inhibitor molecules and nitrate ions present in the acidic medium. Such deviations are commonly observed in adsorption studies involving plant extracts containing multiple active constituents.

The adsorption equilibrium constant (K_{ads}) obtained from the intercept provides information about the strength of adsorption. The comparatively lower values of K_{ads} indicate weaker adsorption affinity of *Mimosa pudica* extract on the brass surface, which is consistent with the moderate inhibition efficiencies observed in gravimetric measurements.

The thermodynamic parameters associated with adsorption, including standard free energy of adsorption (ΔG°_{ads}), are presented in Table 4.

Table 4 Thermodynamic adsorption parameters for green inhibitors on 62/38 brass in 0.75 M HNO₃, showing standard heat of adsorption (Q°_{ads}) and standard free energy of adsorption (ΔG°_{ads}).

Green Inhibitor	Inhibitor Concentration (g L ⁻¹)	Heat of adsorption (Q ^o _{ads}) (kJ mol ⁻¹)		Free energy of adsorption (ΔG ^o _{ads}) (kJ mol ⁻¹)			
		303–313 K	313–323 K	303 K	313 K	323 K	Mean
<i>Mimosa pudica</i> (Lajamani)	0.50	-25.10	-20.50	-18.95	-19.55	-20.15	-19.55
	0.75	-26.90	-22.25	-19.85	-20.46	-21.07	-20.46
	1.00	-28.85	-24.10	-20.95	-21.57	-22.18	-21.57
	1.25	-30.70	-25.90	-21.95	-22.58	-23.20	-22.58
	1.50	-32.60	-27.75	-23.05	-23.69	-24.32	-23.69

The values of ΔG^o_{ads} are negative over the studied temperature range, confirming that the adsorption process is spontaneous. The magnitude of ΔG^o_{ads} varies from approximately **-18.95 to -24.32 kJ mol⁻¹** with increasing inhibitor concentration.

The relatively low magnitude of ΔG^o_{ads} (less than -40 kJ mol⁻¹) indicates that adsorption occurs predominantly through physical interaction between inhibitor molecules and the metal surface. The adsorption is therefore governed mainly by electrostatic interaction between protonated phytochemical species and the charged metal surface. The heat of adsorption (Q^o_{ads}) values are also negative, indicating an exothermic adsorption process. The magnitude of Q^o_{ads} increases with increasing inhibitor concentration, suggesting stronger interaction at higher surface coverage, although the interaction remains within the range characteristic of physisorption.

The relatively moderate values of ΔG^o_{ads} and Q^o_{ads} explain the observed decrease in inhibition efficiency at higher temperatures and higher acid concentrations, as the adsorbed inhibitor layer lacks sufficient stability under aggressive conditions.

Overall, the adsorption analysis confirms that *Mimosa pudica* extract inhibits corrosion of brass in nitric acid through an adsorption-controlled mechanism following Langmuir isotherm behaviour. However, the adsorption strength is limited, resulting in moderate inhibition efficiency and reduced performance under highly aggressive conditions.

3.4 Thermodynamic Considerations

The thermodynamic parameters obtained from temperature and adsorption studies provide insight into the nature of the inhibitor film formed by *Mimosa pudica* extract on the brass surface.

The negative values of ΔG^o_{ads}, discussed in Section 3.3, confirm that the adsorption process is spontaneous. The magnitude of ΔG^o_{ads} (-18.95 to -24.32 kJ mol⁻¹) indicates that adsorption occurs predominantly through physical interaction.

The increase in activation energy (Section 3.2) in the presence of inhibitor suggests the formation of an energy barrier that reduces metal dissolution. However, the moderate values of E_a indicate weak interaction between inhibitor molecules and the metal surface.

The decrease in inhibition efficiency with increasing temperature further supports a physisorption mechanism, where adsorbed molecules tend to desorb at elevated temperatures.

Overall, the inhibition of brass corrosion by *Mimosa pudica* extract is governed by an adsorption-controlled process involving predominantly physical interaction, resulting in moderate film stability.

3.5 Electrochemical Studies (Potentiodynamic Polarization)

The electrochemical behaviour of 62/38 brass in 0.75 M HNO₃ in the absence and presence of *Mimosa pudica* (Lajamani) extract was investigated using potentiodynamic polarization measurements. The electrochemical parameters, including corrosion

potential (E_{corr}), corrosion current density (I_{corr}), and Tafel slopes (β_a and β_c), are presented in Table 5.

Table 4.1.12 Electrochemical polarization parameters of 62/38 brass in 0.75 M HNO₃ in the absence and presence of *Mimosa pudica* inhibitor, including corrosion potential (E_{corr}), corrosion current density (I_{corr}), Tafel slopes (β_a and β_c), and inhibition efficiency determined by polarization and weight loss methods.

Green inhibitor	E_{corr} (mV)	Corrosion current density from intersection of anodic and cathodic tafel line I_{corr} ($\mu A cm^{-2}$)	Tafel slope (V/decade)			Inhibition efficiency IE (%) calculated from	
			β_a (V dec ⁻¹)	β_c (V dec ⁻¹)	β (V)	Polarization method	Weight loss method
Blank	-297.00	38.82	0.074	0.165	0.0222	—	—
<i>Mimosa pudica</i> (Lajamani)	-270.00	22.08	0.100	0.240	0.0312	48.74	53.64

The corresponding polarization curves for the blank and inhibited systems are shown in Figure 5.

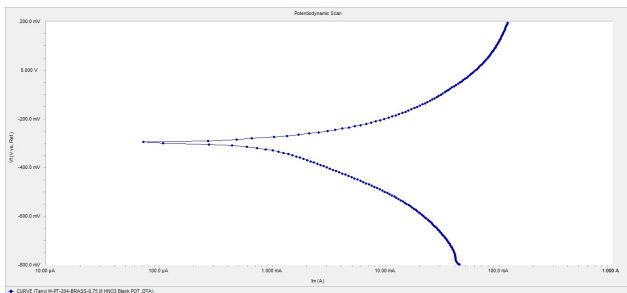


Figure 5a Potentiodynamic polarization curve of 62/38 brass in 0.75 M HNO₃ solution (blank) at 303 K.

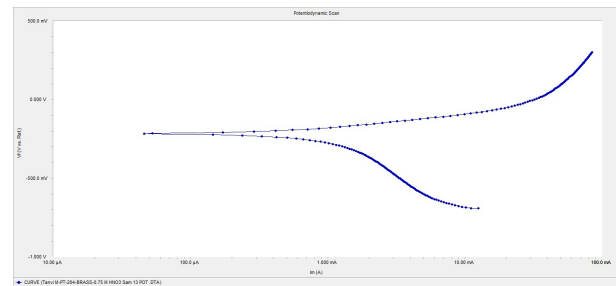


Figure 5b Potentiodynamic polarization curves of 62/38 brass in 0.75 M HNO₃ in the absence and presence of 1.50 g L⁻¹ *Mimosa pudica* seed extract at 303 K.

In the absence of inhibitor, the polarization curve exhibits a higher corrosion current density, indicating rapid dissolution of brass in nitric acid medium. Upon addition of *Mimosa pudica* extract, a decrease in corrosion current density (I_{corr}) is

observed, confirming inhibition of the corrosion process.

The reduction in I_{corr} indicates the formation of an adsorbed film on the metal surface, which restricts charge transfer reactions and reduces the rate of

corrosion. However, the decrease in corrosion current density is moderate, which is consistent with the inhibition efficiencies obtained from weight loss measurements.

The corrosion potential (E_{corr}) shows only a slight shift in the presence of inhibitor, indicating that the inhibitor does not significantly alter the corrosion mechanism. The variation in both anodic (β_a) and cathodic (β_c) Tafel slopes suggests that the inhibitor influences both anodic metal dissolution and cathodic reactions.

Based on these observations, *Mimosa pudica* extract can be classified as a mixed-type inhibitor, as it affects both anodic and cathodic processes without causing a significant displacement in corrosion potential.

The inhibition efficiency calculated from polarization data follows the same trend as that obtained from gravimetric measurements, confirming the reliability and consistency of the experimental results.

Overall, the polarization study supports that corrosion inhibition occurs through adsorption of inhibitor molecules on the brass surface, forming a partially protective layer that reduces the rate of electrochemical reactions.

3.6 Surface Characterization Studies (SEM, AFM and FTIR)

Surface characterization of 62/38 brass specimens immersed in 0.75 M HNO_3 in the absence and presence of *Mimosa pudica* (Lajamani) extract was carried out using scanning electron microscopy (SEM), atomic force microscopy (AFM), and Fourier transform infrared spectroscopy (FTIR) to evaluate the nature of the protective film formed on the metal surface.

3.6.1 SEM Analysis

The SEM micrographs of the brass surface before and after immersion in the corrosive medium are shown in Figure 6.

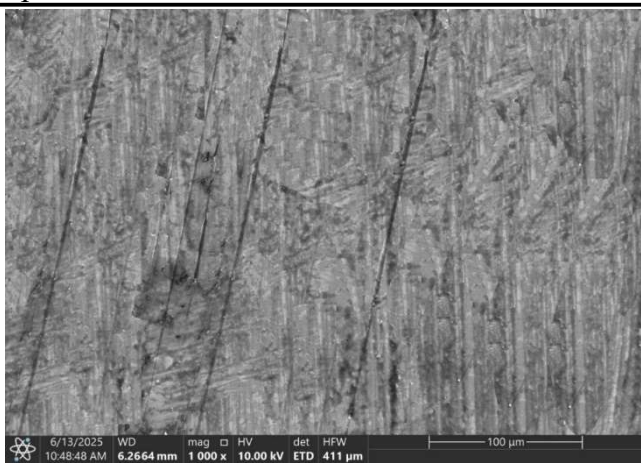


Figure 6a SEM micrograph of polished 62/38 brass surface before immersion.

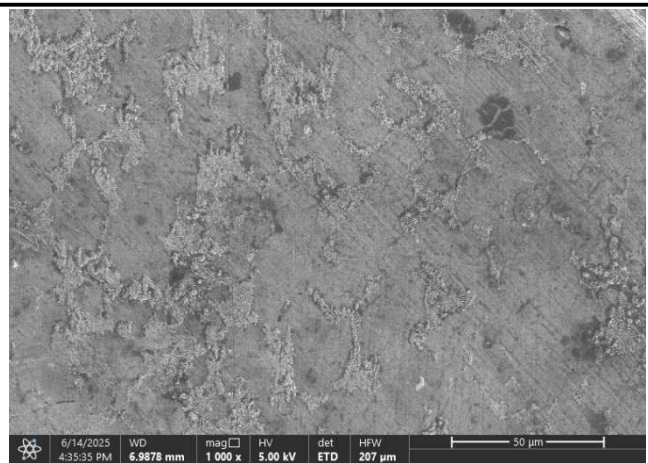


Figure 6b SEM micrograph of 62/38 brass surface after immersion in 0.75 M HNO_3 (blank) at 303 K for 24 h.

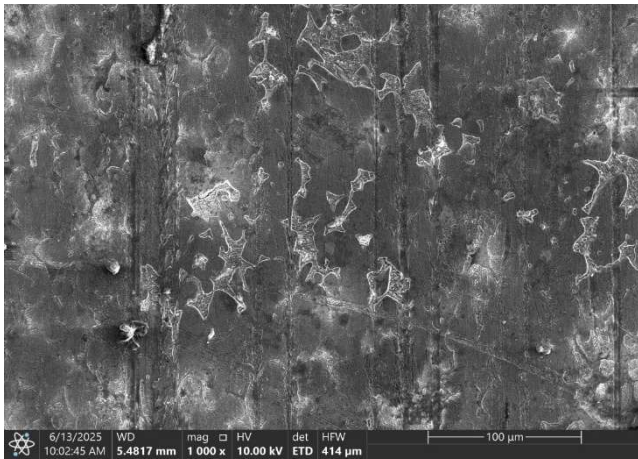


Figure 6c SEM micrograph of 62/38 brass surface after immersion in 0.75 M HNO₃ in the presence of 1.50 g L⁻¹ *Mimosa pudica* seed extract at 303 K for 24 h.

The polished brass surface exhibits a relatively smooth morphology with minor surface irregularities. In contrast, the surface exposed to

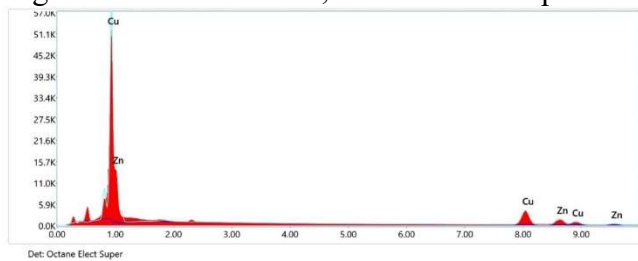


Figure 7a EDX spectrum of polished 62/38 brass surface before immersion.

nitric acid in the absence of inhibitor shows severe damage, characterized by pits, cracks, and non-uniform corrosion features, indicating aggressive dissolution of the metal.

In the presence of *Mimosa pudica* extract, the surface morphology appears comparatively smoother with significantly reduced corrosion damage. The reduction in surface roughness and absence of deep pits suggest the formation of a protective adsorbed layer on the metal surface.

However, the surface is not completely uniform, indicating that the protective film is not fully compact, which is consistent with the moderate inhibition efficiency observed in gravimetric and electrochemical studies.

3.6.2 EDX Analysis

The elemental composition of the brass surface was analysed using EDX, and the corresponding spectra are shown in Figure 7, while quantitative elemental data are presented in Table 6.

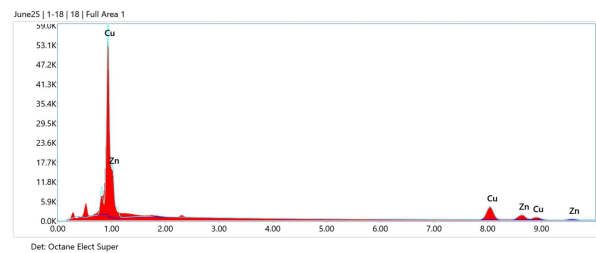


Figure 7b EDX spectrum of 62/38 brass surface after 24 h immersion in 0.75 M HNO₃ (blank).

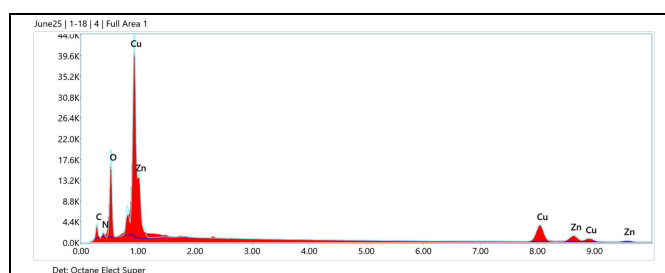


Figure 7c EDX spectrum of 62/38 brass surface after 24 h immersion in 0.75 M HNO₃ containing 1.50 g L⁻¹ *Mimosa pudica* seed extract.

Table 6 Percentage of elements present on the 62/38 brass surface obtained from EDX spectrum analysis.

Green Inhibitor	Cu (%)	Zn (%)	C (%)	N (%)	O (%)	S (%)	Cl (%)	P (%)
Polished Brass	62.00	38.00	0.00	0.00	0.00	0.00	0.00	0.00
Blank	59.70	40.30	0.00	0.00	0.00	0.00	0.00	0.00
<i>Mimosa pudica</i> (Lajamani)	44.40	25.30	13.20	1.80	15.30	0.00	0.00	0.00

The EDX spectrum of the uninhibited sample shows strong signals corresponding to copper (Cu) and zinc (Zn), along with the presence of oxygen, indicating oxide formation due to corrosion.

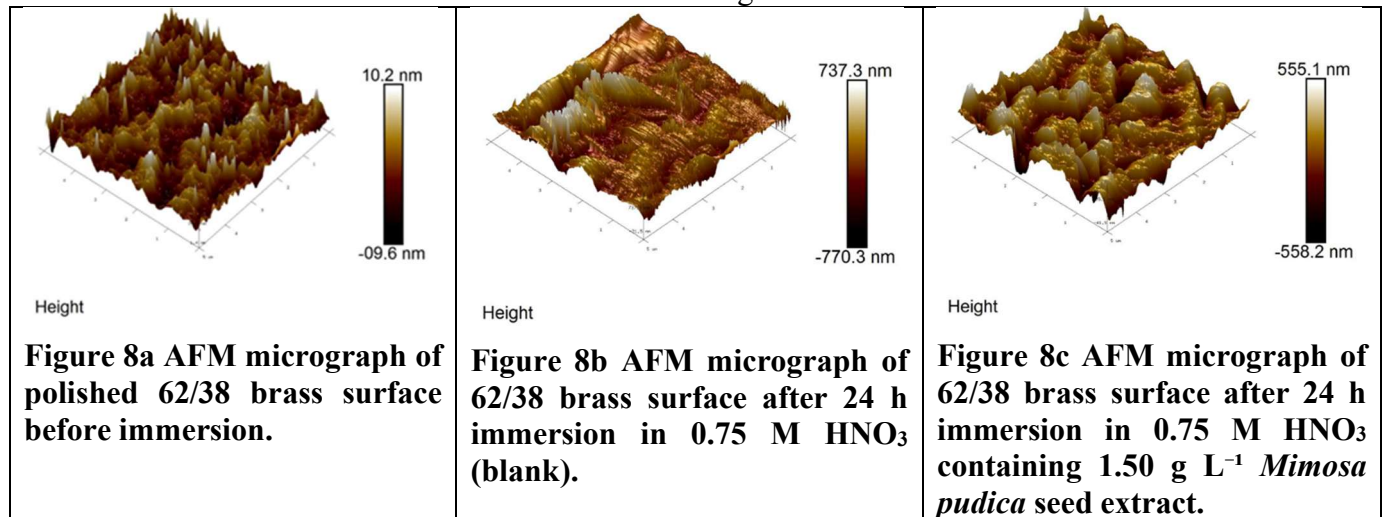
In the presence of *Mimosa pudica* extract, changes in elemental composition are observed. A relative decrease in oxygen content is noted, indicating reduced oxidation of the metal surface. Additionally, the appearance or increase in signals corresponding to elements such as carbon and oxygen associated

with organic compounds confirms the adsorption of inhibitor molecules on the brass surface.

These observations support the formation of an adsorbed organic layer that acts as a barrier against corrosive attack. However, the changes are moderate, suggesting partial surface coverage rather than complete protection.

3.6.3 AFM Analysis

The surface topography of brass specimens was analysed using AFM, and the images are shown in Figure 8.



The uninhibited sample shows a rough and irregular surface with high peak-to-valley variations, indicating severe corrosion. In contrast, the inhibited sample exhibits reduced surface roughness and a relatively smoother morphology.

The decrease in roughness parameters such as average roughness (R_a) and root mean square roughness (R_q) confirms the formation of a protective layer. However, the reduction is not drastic, indicating that the film is not completely uniform.

3.6.4 FTIR Analysis

The FTIR spectra of the *Mimosa pudica* extract and the adsorbed film are shown in Figure 9.

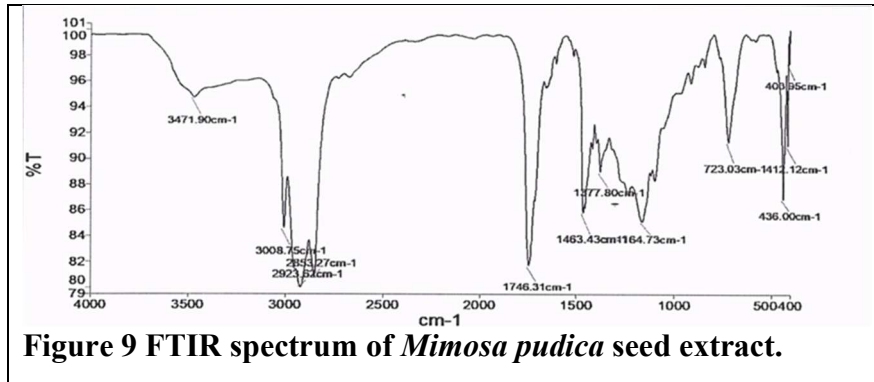


Figure 9 FTIR spectrum of *Mimosa pudica* seed extract.

The spectrum of the pure extract shows characteristic peaks corresponding to functional groups such as O–H, N–H, C=O, and C–O. After adsorption, slight shifts in peak positions and changes in intensity are observed, indicating interaction between these functional groups and the metal surface.

The absence of significant new peaks suggests that adsorption occurs primarily through physical interaction rather than strong chemical bonding.

Overall Interpretation

The combined SEM, EDX, AFM, and FTIR analyses confirm that *Mimosa pudica* extract adsorbs onto the brass surface, forming a protective layer that reduces corrosion.

However, the morphological features, moderate reduction in roughness, and limited compositional changes indicate that the protective film is not highly compact or strongly bound. This is consistent with the physisorption mechanism and moderate inhibition efficiency observed from gravimetric and electrochemical studies.

CONCLUSION

The corrosion behaviour of 62/38 brass in nitric acid and its inhibition by *Mimosa pudica* (Lajamani) extract were evaluated using gravimetric, electrochemical, adsorption, and surface characterization techniques.

The inhibition efficiency increased with increasing inhibitor concentration and decreased with

increasing acid concentration and temperature. The maximum inhibition efficiency was observed at higher inhibitor concentration under lower acid strength conditions.

Adsorption of the inhibitor followed the Langmuir adsorption isotherm, indicating monolayer formation on the metal surface. The negative values of ΔG°_{ads} confirmed spontaneous adsorption, with magnitude indicating predominantly physical interaction.

The increase in activation energy in the presence of inhibitor and the decrease in inhibition efficiency with temperature further supported a physisorption mechanism.

Potentiodynamic polarization studies showed a decrease in corrosion current density with slight shift in corrosion potential, indicating that *Mimosa pudica* extract acts as a mixed-type inhibitor.

Surface characterization studies using SEM, EDX, AFM, and FTIR confirmed the formation of an adsorbed protective layer on the brass surface. However, the film was not fully compact, which explains the moderate inhibition efficiency.

Overall, *Mimosa pudica* extract acts as a concentration-dependent, adsorption-controlled corrosion inhibitor for brass in nitric acid, with moderate effectiveness governed by predominantly physical adsorption.

ACKNOWLEDGMENT

The authors thank the Chemistry Department, Sir P. T. Sarvajani College of Science, Surat, for providing laboratory facilities. The authors also acknowledge the Department of Chemistry at The Maharaja Sayajirao University of Baroda for access to the electrochemical workstation used for polarisation measurements. AFM analysis was carried out at the Materials Research Centre (MRC), Malaviya National Institute of Technology (MNIT), Jaipur, and the authors gratefully acknowledge the facility support.

REFERENCES

- [1] A. S. Fouda, G. Y. Elewady, and A. S. Abousalem, "Corrosion inhibition of copper and its alloys in nitric acid solutions using organic compounds," *J. Bio- Tribo-Corros.*, vol. 7, p. 45, 2021.
- [2] L. Guo, S. Zhu, S. Zhang, Q. He, and W. Li, "Corrosion inhibition of copper in acidic media using plant extracts: A review," *Corros. Sci.*, vol. 164, p. 108334, 2020.
- [3] M. A. Quraishi, D. S. Chauhan, and V. S. Saji, "Heterocyclic compounds as green corrosion inhibitors for metals in acidic media," *J. Mol. Liq.*, vol. 321, p. 114641, 2021.
- [4] N. K. Gupta, C. Verma, and M. A. Quraishi, "Plant extracts as green corrosion inhibitors for metals in acid environments," *J. Mol. Liq.*, vol. 315, p. 113707, 2020.
- [5] D. Verma, E. E. Ebenso, and M. A. Quraishi, "Recent advances in corrosion inhibition using plant extracts," *J. Mol. Liq.*, vol. 322, p. 114805, 2021.
- [6] S. A. Umoren and M. M. Solomon, "Recent developments on the use of plant extracts as corrosion inhibitors," *J. Environ. Chem. Eng.*, vol. 10, p. 107456, 2022.
- [7] C. Verma, E. E. Ebenso, I. Bahadur, and M. A. Quraishi, "An overview on plant extracts as corrosion inhibitors for metals," *J. Mol. Liq.*, vol. 310, p. 113151, 2020.
- [8] H. Lgaz, R. Salghi, K. S. Bhat, and I. H. Ali, "Electrochemical and surface studies of corrosion inhibition using plant-based compounds," *J. Mol. Liq.*, vol. 330, p. 115703, 2021.
- [9] P. Mourya, S. Banerjee, and M. M. Singh, "Corrosion inhibition using natural products: Mechanistic insights," *Corros. Sci.*, vol. 172, p. 108693, 2020.
- [10] A. K. Singh and M. A. Quraishi, "Effect of plant extract as corrosion inhibitor for metals in acidic medium," *J. Taiwan Inst. Chem. Eng.*, vol. 107, pp. 195–205, 2020.
- [11] M. Finšgar and J. Jackson, "Application of corrosion inhibitors for steels in acidic media: A review," *Corros. Sci.*, vol. 152, pp. 123–133, 2019.
- [12] I. B. Obot and N. O. Obi-Egbedi, "Adsorption and inhibitive properties of eco-friendly inhibitors," *Corros. Sci.*, vol. 165, p. 108386, 2020.
- [13] K. F. Khaled, "Electrochemical investigation of corrosion inhibition behavior," *Electrochim. Acta*, vol. 371, p. 137748, 2021.
- [14] M. A. Deyab, "Green corrosion inhibitors based on plant extracts for metals in aggressive media," *J. Mol. Liq.*, vol. 336, p. 116315, 2021.
- [15] S. A. Umoren and I. B. Obot, "Thermodynamic and kinetic aspects of corrosion inhibition," *Surf. Interface Anal.*, vol. 52, pp. 140–152, 2020.
- [16] A. K. Singh and M. A. Quraishi, "Adsorption behavior and thermodynamic analysis of corrosion inhibitors," *J. Mol. Liq.*, vol. 345, p. 117817, 2022.
- [17] R. Solmaz, "Adsorption and corrosion inhibition properties of natural compounds," *Corros. Sci.*, vol. 182, p. 109256, 2021.
- [18] Y. El Aoufir, H. Lgaz, and R. Salghi, "Electrochemical and surface studies on corrosion inhibition using natural products," *Heliyon*, vol. 6, p. e04672, 2020.
- [19] E. E. Ebenso and M. A. Quraishi, "Green corrosion inhibitors: Theory and practice," *Corros. Rev.*, vol. 39, pp. 1–26, 2021.
- [20] S. A. Umoren and M. M. Solomon, "Plant extracts as corrosion inhibitors for metals in acidic media," *J. Environ. Chem. Eng.*, vol. 10, p. 107456, 2022.
- [21] ASTM G31-72, "Standard practice for laboratory immersion corrosion testing of metals," ASTM Int., West Conshohocken, PA.
- [22] A. J. Bard and L. R. Faulkner, *Electrochemical Methods: Fundamentals and Applications*, 2nd ed. New York, NY, USA: Wiley, 2001.
- [23] J. B. Harborne, *Phytochemical Methods: A Guide to Modern Techniques of Plant Analysis*. Berlin, Germany: Springer, 1998.
- [24] H. H. Uhlig and R. W. Revie, *Corrosion and Corrosion Control*. New York, NY, USA: Wiley, 2008.
- [25] S. Glasstone, K. J. Laidler, and H. Eyring, *The Theory of Rate Processes*. New York, NY, USA: McGraw-Hill, 1941.
- [26] I. Langmuir, "The adsorption of gases on plane surfaces of glass, mica and platinum," *J. Am. Chem. Soc.*, vol. 40, pp. 1361–1403, 1918.
- [27] M. Stern and A. L. Geary, "Electrochemical polarization: A theoretical analysis of the shape of polarization curves," *J. Electrochem. Soc.*, vol. 104, pp. 56–63, 1957.